Polyoxometalate-Single Atom Catalysts (POM-SACs) in Energy Research and Catalysis

Rongji Liu* and Carsten Streb*

Single atom catalysts—SACs—have received intense interest in sustainable energy research due to their enormous application potential and broad catalytic scope. In particular, SACs anchored on molecular metal oxides—polyoxometalates (POMs)—offer unrivalled possibilities as models to understand the function of these complex systems on the atomic level. Research questions which are difficult to address for classical heterogeneous SACs can be addressed by experiment and theory using POM-SACs as prototype catalysts. This review reviews the emerging field of POM-SAC research with a focus on fundamental properties and their application in energy conversion and storage technologies including water splitting, CO/CO₂- as well as N₂-activation. Current limitations of the field are identified and possible routes to overcome these are described. Future areas of development, including polyoxometalate-single-site catalysts, are highlighted, and critically assessed to enable the community to develop this fast-moving field further.

1. Introduction

Metals are one of the most important classes of heterogeneous catalysts. Their applications range from site-selective bond-formation and bond-scission to large-scale industrial catalysis, sustainable energy schemes, and environmental remediation.[1] Over the last century, there has been a continuous drive to optimize the performance of heterogeneous metal catalysts. One main approach is increasing the surface-area-to-volume ratio by decreasing the size of the metal particles. This has led to ever smaller metal particles (including metal nanoparticles ($d >$ 5 nm) and metal nanoclusters ($d \approx 1$ nm)),[1] and finally to single metal atoms as catalytic sites, so-called single atom catalysts, or SACs.[2,3] While metal nanoparticles and nanoclusters have been studied in heterogeneous catalysis for more than 60 years, SACs

have only been explored since the early 21st century, mainly because their identification and characterization has been virtually impossible before, due to a lack of high-resolution instrumentation (such as electron or scanning probe microscopies).[1,4]

Beyond classical heterogeneous SACs, much research has recently focused on developing molecular SAC model systems. Here, polyoxometalate-single atom catalysts (POM-SACs) are of enormous interest as these molecular metal oxides could form the link between molecularly well-defined prototypes and technologically relevant solid-state SACs. In this Review, we will provide a brief introduction into the current status in SACs chemistry. We then discuss pioneering studies as well as current research challenges in POM-SACs chemistry with an emphasis on sustainable energy research. Finally, we will identify future areas in POM-SAC research and highlight the bottlenecks which need to be overcome to further develop this field.

2. Classical Single Atom Catalysts

2.1. Common Anchoring Strategies and Applications of SACs

SACs offer the ultimate atomic reactivity, as each single atom is interacting with its environment and can act as catalytic site.[7–9] The key to the successful preparation of SACs is to stabilize catalytic metal centers as individual atoms by utilizing hosts/supports featuring strong binding motifs (**Figure 1**). Early model systems included high specific surface area carbons,[10,11] metal oxides,[12,13] as well as materials with uniform pores and regular structures, such as zeolites,[14] metal organic frameworks (MOFs)[5,14–19] and covalent organic frameworks (COFs).[20,21] Stabilization of single-atoms on supports requires a support-surface with specific anchoring sites, such as coordinatively unsaturated surface atoms (e.g., O^{2-}, OH^-), surface vacancies or heteroatom dopants (e.g., N, P, S, and halogens). The SACs can be stabilized on the support surface by covalent or ionic interactions, or by geometric enclosure in small pores. Each anchoring mode offers several benefits and challenges. For instance, the coordination of a single metal atom to surface oxo ligands makes the single-atom accessible from the outside, e.g., for binding of a substrate. However, it also leads to high surface-energy and destabilization of the single-atom, so that leaching, or agglomeration are possible. In contrast,
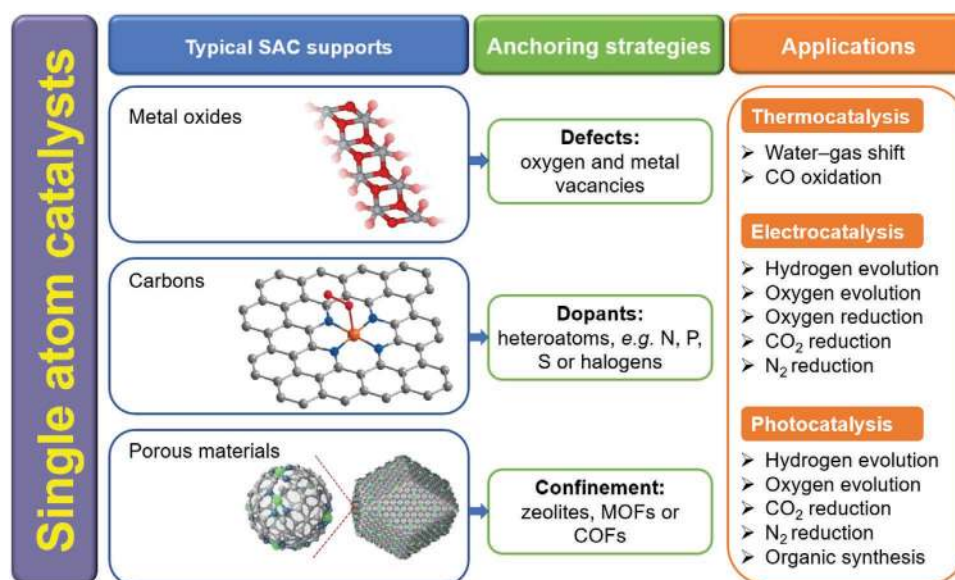
Dr. R. Liu, Prof. C. Streb
Ulm University
Institute of Inorganic Chemistry I
Albert-Einstein-Allee 11, 89081 Ulm, Germany
E-mail: rongji.liu@uni-ulm.de; carsten.streb@uni-ulm.de
Dr. R. Liu, Prof. C. Streb
Helmholtz Institute Ulm
Helmholtzstr. 11, 89081 Ulm, Germany

The ORCID identification number(s) for the author(s) of this article can be found under https://doi.org/10.1002/aenm.202101120.

**ADVANCED
SCIENCE NEWS**
www.advancedsciencenews.com

**ADVANCED
ENERGY
MATERIALS**
www.advenergymat.de

Figure 1. Overview of typical SAC supports, common anchoring strategies, and energy-relevant applications of SACs. Adapted with permission.[5] Copyright 2017, American Chemical Society. Reproduced with permission.[6] Copyright 2017, Wiley-VCH.

single atoms occupying surface vacancy sites feature higher binding energies (and lower risk of leaching/agglomeration); however, the accessibility for interactions with the environment is more restricted. Often, the intricacies of the SAC binding on substrates are difficult to assess, as suitable models to rationalize binding-reactivity correlations are often not accessible.
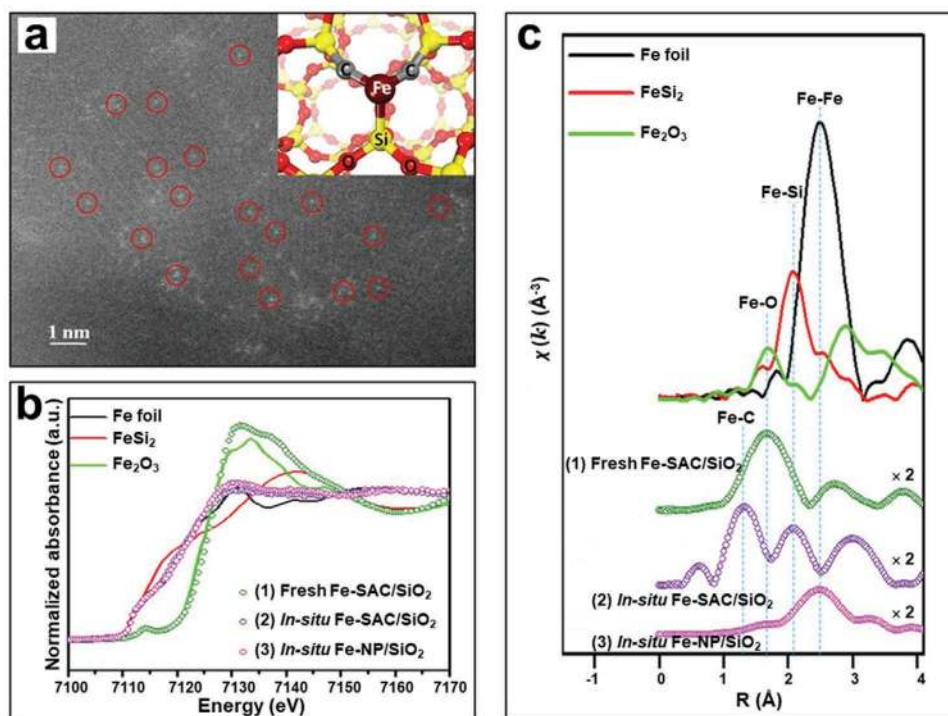
To-date, SACs have been explored in diverse thermo-, electro-, and photocatalytic applications.[22] Pioneering SAC studies were focused on the development of efficient catalysts for energy-relevant thermocatalytic reactions, including the water–gas shift reaction and CO oxidation.[23–25] Over recent years, research has more and more focused on the use of SACs in sustainable energy, including photocatalysis and electrocatalysis.[26–28] In consequence, significant efforts have been put on global bottleneck reactions for carbon-neutral energy schemes, including hydrogen evolution (HER), oxygen evolution (OER), oxygen reduction (ORR), carbon dioxide reduction, and nitrogen reduction.[18,26,29,30] While early studies mainly used noble-metal SACs, more recent work has focused on earth-abundant 3d and 4d transition metal-based SACs. Particularly for electrocatalysis, SACs are typically supported on nitrogen-doped high surface area carbons, where nitrogen-metal coordination bonds are used for SAC anchoring. In a prime example, Tour, Chen and colleagues synthesized single Co atoms anchored to nitrogen-doped graphene (Co−NG) using a pyrolysis approach starting from a Co-salt-impregnated graphene oxide.[31] The formation of isolated Co sites and their anchoring via Co−N−C bonds has been confirmed by X-ray absorption spectroscopy (XAS). These Co-based SACs were identified as active sites for HER in 0.5 M aqueous H_2SO_4, achieving an overpotential (η_{10}) of −146 mV at a current density $j = 10$ mA cm^{-2}. In another ground-breaking example, Li, Wang and colleagues prepared isolated Fe atoms anchored on N-doped porous carbon, using the Fe-doped framework material ZIF-8 as precursor.[6] The resulting SACs showed excellent ORR electroactivity in 0.1 M aqueous KOH solution, with

a half-wave ORR potential ($E_{1/2}$) of 0.90 V versus a reversible hydrogen electrode (RHE), which was nearly 60 mV more positive than a commercial Pt reference catalyst.

SACs also show promising performance in light-driven catalysis. Initially, classical semiconductors, such as TiO_2 and CdS were employed as SAC supports;[32–35] more recently, 2D carbon-based materials with high specific surface area (e.g., carbon nitrides or graphene) have attracted much attention. For instance, Li, Frenkel and colleagues prepared single Co^{2+} sites supported on C_3N_4 via a simple deposition method to give Co-SAC-modified carbon nitrides.[36] The system showed excellent photochemical CO_2 reduction activity and showed high selectivity for CO formation under visible-light irradiation.

2.2. Challenges in SAC Synthesis and Application

Due to the higher surface energy of single metal atoms compared with metal nanoclusters and nanoparticles, SACs are typically highly mobile and tend aggregate under operation.[2,37–39] This poses challenges and limitations for both synthesis and subsequent application. One strategy to overcome this, is to operate in highly dilute conditions and decrease the metal loading to levels below 1 wt%; this however limits the overall activity of the system due to the low number of SACs present. Another challenge in the field is the lack of understanding of SAC-substrate interactions and binding modes, as often SACs are deposited at substrate surface defects. This makes experimental and theoretical rationalization of reactivity difficult and prevents structure–reactivity correlations. Prime examples for these challenges are SACs anchored on (metal-)oxides, where structural defects or low crystallinity can result in unclear binding situations. A ground-breaking study on SACs anchored on metal oxides was reported by Zhang, Li, Liu and co-workers. The authors synthesized FeO_x-supported single Pt atoms (0.17 wt% Pt-SAC/FeO_x) using a coprecipitation method, leading

**ADVANCED
SCIENCE NEWS**

www.advancedsciencenews.com

**ADVANCED
ENERGY
MATERIALS**

www.advenergymat.de

Figure 2. Structural features of the SAC 0.5% Fe-SAC/SiO$_2$. a) STEM-HAADF image of the catalyst after reaction, with the inset showing the computational model of the single iron atom bonded to two C atoms and one Si atom within a silica matrix. b) In situ XANES spectrum after catalyst activation and c) Fourier transformed (FT) k^3-weighted $\chi(k)$-function of the EXAFS spectrum. Solid lines denote reference samples (Fe foil, FeSi$_2$, and F$_{e2}$O$_3$). (1) marks the fresh 0.5% Fe-SAC/SiO$_2$; (2) marks in situ formed Fe-SACs in 0.5% Fe-SAC/SiO$_2$; (3) marks in situ 0.5% Fe-NP/SiO$_2$ (iron NPs supported on SiO$_2$) upon activation in 10% CH$_4$/N$_2$ at 1173 K for 2 h, respectively. Reproduced with permission.[40] Copyright 2014, American Association for the Advancement of Science.

to a highly active CO oxidation catalyst.[24] Comprehensive characterization methods including high-angle annular dark-field scanning transmission electron microscopy (HAADF-STEM), X-ray absorption near-edge structure/extended X-ray absorption fine structure spectroscopy (XANES/EXAFS), Fourier-transform infrared spectroscopy studies of CO adsorption revealed that the positively charged single Pt atoms occupy vacant iron atom lattice positions. Density functional theory (DFT) calculations indicated that the Pt atoms were most probably located at the threefold hollow site on the O$_3$-terminated surface of FeO$_x$, which is consistent with experimental data. The DFT calculations also indicated that the high catalytic activity of Pt-SAC/FeO$_x$ correlates with the partially vacant 5d orbitals of the positively charged Pt atoms, which reduce both the CO adsorption energy and the activation barriers for CO oxidation. In a later seminal example, Bao and colleagues used an iron-SAC deposited on amorphous silica (0.5 wt% Fe-SAC/SiO$_2$) for the selective C−H activation of methane to give value-added products, such as alkenes and aromatic compounds. The iron species are redistributed from the original iron oxide (Fe$_2$O$_3$/Fe$_3$O$_4$) NPs to isolated atoms during catalyst activation (**Figure 2**). The study beautifully demonstrates the immense challenges and efforts required to understand structure, bonding, and reactivity of the SAC surface sites.[40] In another example, single Au atoms supported on CeO$_2$ (Au loading: 0.05 wt%) were prepared by Liu, Zhang, Li and co-workers. The group demonstrated that the system has a high selectivity for preferential CO oxidation over H$_2$ oxidation when operated in CO/H$_2$ mixtures in the pres-

ence of O$_2$.[41] This ability is critical for providing high-purity H$_2$ (by oxidative removal of CO), e.g., for fuel cells. As next step, it would be important to fully understand the atomic causes for this behavior and utilize this to access designer SACs with tuneable reactivity and selectivity.

In addition to metal oxides, N-doped carbons are a widely studied support for SACs. This is due to their proposed "N$_4$" binding sites based on four coordinating nitrogen donors which are suitable for coordinating a wide range of single metal atoms. In a seminal study, Chen and co-workers synthesized single-atom Fe−N$_4$ motifs on N-doped porous carbon using a polymerization–pyrolysis–evaporation strategy.[42] Electrocatalytic studies showed that the material features a low OER overpotential of $\eta_{10} = 0.43$ V. Based on experimental data and DFT calculations, the authors attributed this to the Fe−N$_4$ configuration which enabled a low free energy barrier for the rate-determining OER step (i.e., the O−O bond formation). Consequently, reference materials without this Fe−N$_4$ binding motif showed significantly lower OER catalytic performance.

These studies highlight, that progress in the field could be significantly enhanced by combined experimental and theoretical studies on small, well-defined model systems to rationalize general principles of SAC design and function. For these reasons, the design of SACs models with atomically well-defined single metal atom binding sites would be immensely important for the field, so that structure–property-function relationships can be established, and theoretical predictions on reactivity can be verified by easily accessible model systems.[10,43]

**ADVANCED
SCIENCE NEWS**
www.advancedsciencenews.com

**ADVANCED
ENERGY
MATERIALS**
www.advenergymat.de

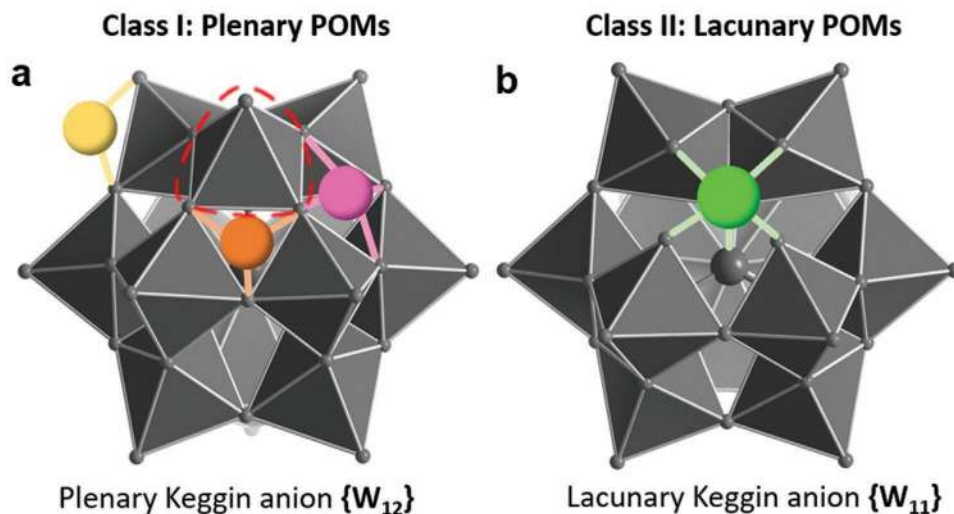## 3. From Heterogeneous to Molecular SAC Supports: Polyoxometalate-Anchored SACs

Molecular metal oxides, or POMs, are ideal model systems to explore structure and function of metal-oxide-anchored SACs. POMs are atomically well-defined polynuclear metal oxide anions which can be considered molecular analogues of solid-state metal oxides.[44,45] POMs combine technologically important reactivities of solid-state oxides with the structural and chemical tunability of molecules. This has led to varied applications in (electro- and photo-)catalysis[46,47] molecular electronics[48,49] and nanomaterials.[50]

POMs are ideal molecular systems to explore the anchoring of SACs, as the POM-surface is formed by terminal (M=O) and bridging (e.g., M−O−M) groups, where coordinative binding of metal centers is possible.[51,52] As illustrated in **Figure 3**a, a range of coordination sites with different all-oxo coordination environments are accessible on the surface of the prototype (so-called plenary) Keggin anion $[XM_{12}O_{40}]^{n-}$ (X, e.g., B, Si, P; M typically Mo, W, hereafter, we use X = P, M = W as model: $[PW_{12}O_{40}]^{3-}$ {**W12**}).[52] This includes linear (coordination number CN = 2), trigonal (CN = 3), and tetragonal (CN = 4) sites. These sites are essentially identical with typical SAC binding sites on classical solid-state metal oxides. In addition, controlled hydrolysis of POMs is possible, enabling selective removal of one or several "M = O" units, giving so-called lacunary clusters, e.g., $[PW_{11}O_{39}]^{7-}$ (= {**W11**}, Figure 3b). In these species, SACs can also be anchored into the framework of the POM rather than to the POM surface. These isolated binding sites form "coordination islands" which are ideally suited for permanent single metal atom coordination and limit leaching and loss of the metal centers.[52] Each of these sites feature different physical and electronic structures and thus, reactivities. In addition, the strong electronic support-SAC interactions (electrostatic and coordinative) can be used to selectively tune

the chemistry of the SACs for specific processes. For example, chemical modification of the POM-structure and elemental composition can be used to control redox potentials or binding site structures, so that SAC-support-interactions can be studied based on experimentally accessible models.[53] In addition, the well-defined molecular structure of POMs makes them ideal systems for computational studies and reactivity prediction.[54] Also, POMs offer multifunctionality and combine redox- and photoactivity with tunable Bronsted and Lewis acidity/basicity. These features can be coupled with the properties of the SAC to access synergistic reactivity. Finally, while most POM-SAC studies have been focused on Keggin-anions derivatives, it should be noted that POM-SACs can principally be formed by all POMs, so that a vast area of research is accessible for experimental and theoretical studies. Possible target applications include (photo-/electro-/thermal) catalysis as well as energy conversion/storage.

Based on these promising features and driven by the fast-paced progress in SAC development for challenging catalyses, recent years have seen pioneering theoretical and experimental studies to establish the new field of POM-SAC chemistry.

In this Review, we summarize pioneering studies which lay the foundations for the field, we highlight current areas where progress has been made, and we identify future directions where POM-SACs could become unique catalytic prototypes and model systems. This includes thermal, electrochemical, and light-driven catalysis together with applications in energy conversion/storage. We describe how POM-supports could be unique systems for stabilizing SACs and thereby prevent agglomeration, leaching, and catalyst deactivation. In addition, based on the current mechanistic understanding, we propose new approaches to control SAC reactivity by tuning the structure of the POM-support as well as the POM-SAC interactions. We expect these features to enable new reactivity for challenging multielectron redox catalyses.

Class I: Plenary POMs   **Class II: Lacunary POMs**

Plenary Keggin anion {**W12**}   Lacunary Keggin anion {**W11**}

Figure 3. Classification of POM-SACs together with an illustration of prototypical binding sites and coordination modes. a) Class I POM-SACs: SAC binding sites in the plenary Keggin anion $[XM_{12}O_{40}]n^-$ (= {**W12**}). b) Class II POM-SACs, highlighting the additional metal binding site in a lacunary Keggin anion $[XM_{11}O_{39}]m^-$ (= {**W11**}).[52] SAC sites indicated in a) can be described as surface sites, whereas the SAC site in b) results from metal substitution within the Keggin metal oxide framework. Note that {**W11**} is formed by hydrolytic removal of a "W = O" group from {**W12**} (marked in a) by a red dashed circle).

3.1. Nomenclature and Definition of POM-SACs

SAC research is at the interface between molecular and solid-state chemistry, and SAC design is targeted by a range of approaches from a wide array of research areas. As such, SAC nomenclature can be somewhat vague at times; for clarity, we define the term POM-SAC as a molecular system, where a single metal atom is anchored to the POM surface or embedded in the POM framework (see Figure 3 for distinction between surface-anchoring and framework-embedding). These species are chemically distinct to other literature-known materials classes, including

- Classical SACs, where a metal atom is anchored to a heterogeneous support (e.g., carbon or a metal oxide). Note that in these materials, the single metal atoms can be in different chemical environments due to the presence of different binding sites on the support.
- Single-site heterogeneous catalysts (SSHCs), where single, identical reaction sites (composed of one or several atoms) are located in well-defined positions on a heterogeneous, typically porous support.[55]

Based on structural and chemical considerations, we propose to divide POM-SACs into two sub-classes:

Class I POM-SACs are based on plenary POM clusters, where the cluster shell is complete, (i.e., no metal-oxo units have been hydrolytically removed),[52] and the SAC binds to the outside of the cluster, typically in geometrically predefined positions in an all-oxo environment (Figure 3a).

Class II POM-SACs are based on so-called lacunary POM anions where one or several metal-oxo units have been removed from the cluster shell, thus creating vacant metal binding sites where the SAC can be coordinated in an all-oxo environment (Figure 3b). In the following sections, we will explore similarities and differences between both classes, and highlight areas where each class can have major impact on future developments in the field.
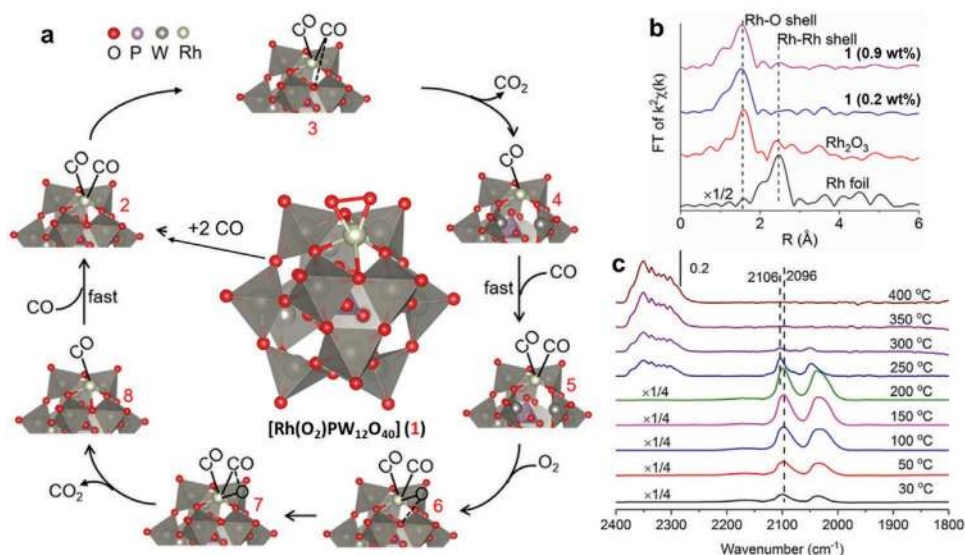
3.2. Noble-Metal-Functionalized POM-SACs

Class I systems: The embedding of noble metal cations in POMs has become feasible using self-assembly- or selective ion insertion-routes, and has been described in several reviews.[56,57] Pioneering work in noble metal based Class I POM-SACs systems was started by the Yan group in 2016.[58] To-date, the exploration of Class I POM-SACs featuring single noble-metal atoms is still in its infancy, and most studies have focused on the plenary Keggin-ion $[XM_{12}O_{40}]^{n-}$ with the SAC bound to the cluster surface (Figure 3a).[53,58–60]

In an early study from 2016, Yan and co-workers reported the site-specific surface-anchoring of individual Pt atoms on phosphomolybdic acid ($[H_3PMo_{12}O_{40}]$) clusters supported on activated carbon, resulting in Class I POM-SACs. The authors reported a high Pt metal loading of ≈1 wt% and demonstrated the use of their composite for hydrogenation catalysis.[58] Structural information on the system was obtained by detailed XAS: EXAFS analyses highlighted the absence of short-range Pt–Pt-interactions (as expected for Pt metal aggregates), indicating the presence of single Pt atoms, which was also confirmed by transmission electron microscopy analysis. Further, comparative EXAFS and Fourier transform spectral analyses showed strong resemblance of the system studied by the authors with the molecular reference complex $[Pt(acac)_2]$ (acac – acetylacetonate), where a positively charged Pt atom is located in a square planar coordination environment. This led the authors to propose that their system features individual Pt atoms located in the square position (4-H site) on the Keggin anion surface (Figure 3a, pink sphere). DFT calculations provided further evidence that this location is the most stable coordination site for the Pt atom. In the field of SACs, the main challenge for DFT analyses is the appropriate modeling of the support surface, as the exact SAC binding mode is often not well understood. In contrast, for POM-SACs, the molecular structure of the POM-support is typically well known from single-crystal XRD studies, so that suitable structural POM-SAC models can be provided for advanced calculations. Several groups have used this metal-functionalized POM-SAC model system (where the SAC is located in the 4-H site) for computational studies on reduction/oxidation reactions including alkene epoxidation,[61] N_2 reduction,[62,63] NO_x (NO and N_2O) reduction,[64–66] and CO oxidation.[67–70]

In 2019, Sautet, Yan and co-workers investigated how metal-support interactions affect stability and hydrogenation activity of Class I POM-SACs. To this end, they compared the binding of Pt atoms on four Keggin-anions, $[XM_{12}O_{40}]^{n-}$ (X = P (n = 3), Si (n = 4), M = W^{VI}, Mo^{VI}) using experiment and theory.[60] DFT-computations on the systems showed, that the Pt adsorption energies ($E_{ads,Pt}$, for binding to the square-planar surface site, Figure 3a, pink sphere) varied by nearly 2 eV between the four POM-supports studied. The authors used this understanding to explain why the system with low Pt adsorption energy ($[PW_{12}O_{40}]^{3-}$, $E_{ads,Pt}$ ≈5 eV), showed formation of Pt nanoparticles ($E_{cohesion,Pt}$ = 5.5 eV)). In contrast, the POMs where $E_{ads} > E_{cohesion,Pt}$ provided suitable sites to stabilize individual positively charged Pt atoms.

In the area of CO-activation, Yan and co-workers proposed that Rh-containing POM-SACs could show synergistic oxidative reactivity. To this end, the authors synthesized a Rh-containing POM-SAC with the proposed formula $[Rh(O_2)PW_{12}O_{40}]$) and investigated its CO oxidation performance (**Figure 4**).[59] In systematic experimental studies, the authors proposed an involvement of the POM-based surface oxygen species as oxidant for the catalytic conversion of CO to CO_2, at elevated temperatures (between 150 and 400 °C). Evidence was provided by in situ diffuse reflectance infrared Fourier transform (DRIFT) spectroscopy which indicated that specific POM oxo ligands (located adjacent to the Rh atom, see Figure 4a) react with CO adsorbed on the Rh single atom to give CO_2. The surface oxygen vacancy is subsequently filled by O_2-based reoxidation. In essence, this results in a complete catalytic cycle with a typical Mars–van Krevelen (MvK) mechanism. In a follow-up study, the group provided experimental observations of the changes of the catalytic key components, i.e., the Rh center, the POM-support, and the CO-substrate, by using a combination of operando XAS, in situ XPS, and DRIFT techniques, which highlighted that reoxidation of the POM-support is the rate-determining step.[53] This SAC/POM-support synergism was further studied by using

**ADVANCED
SCIENCE NEWS**

www.advancedsciencenews.com

**ADVANCED
ENERGY
MATERIALS**

www.advenergymat.de

Figure 4. Use of Class I POM-SACs ([Rh(O$_2$)PW$_{12}$O$_{40}$], **1**) for CO oxidation. a) Proposed CO oxidation mechanism for catalyst **1**. b) k^2-weighted Rh K-edge EXAFS spectra of **1** (containing 0.2 or 0.9 wt% Rh), and the reference compounds Rh foil and Rh$_2$O$_3$. c) In situ DRIFT spectra of **1** (containing 0.9 wt% Rh) in the presence of CO and O$_2$ flow at various temperatures. Adapted with permission.[59] Copyright 2017, American Chemical Society.

three other Keggin-type POMs ([SiW$_{12}$O$_{40}$]$^{4-}$, [PMo$_{12}$O$_{40}$]$^{3-}$, [SiMo$_{12}$O$_{40}$]$^{4-}$) featuring different oxidation potentials. This comparative analysis showed that the activity of the four Rh-POM-SACs follow the mechanistic suggestions; the POM-SAC with the lowest oxidation potential (i.e., [PMo$_{12}$O$_{40}$]$^{3-}$) shows the highest catalytic activity, highlighting that predictive correlations between experimentally accessible data and reactivity are possible for POM-SACs.

Initial studies suggested a MvK mechanism for the CO oxidation by Rh-functionalized POM-SACs. However, subsequent DFT analyses revealed that an alternative Langmuir–Hinshelwood mechanism could be energetically favoured.[70] To gain insight into this discrepancy, Liu and colleagues performed DFT calculations to show that the oxo ligands bound to the single-atom site are chemically nonequivalent, due to polarization effects of the anchored SAC. When these effects are considered in the mechanistic analysis,[69] theory again predicts that the MvK mechanism is energetically favored for the Rh-functionalized POM-SACs studied. Similar reactivity differences of surface oxygens were also reported by Liu and co-workers based on DFT-studies of the reduction of NO and N$_2$O by CO for a number of POM-SACs.[64,65] The result shows that the MvK mechanism is energetically favoured for CO oxidation and is suggested to proceed by formation of an oxygen vacancy on the POM surface, while NO or N$_2$O act as an oxygen atom donor to replenish the oxygen vacancy on the POM and release N$_2$. These studies show that detailed understanding of reaction mechanisms together with high-level DFT analyses can be used to control and predict SAC/POM-support interactions. This enables researchers to modulate catalytic reactivity based on understanding of the physical/chemical properties of the POM.

Class II systems: In an early study on Ru-containing POM-SACs, Neumann and colleagues employed the mono-Ru-functionalized lacunary Keggin-species [Ru^{III}(H$_2$O)SiW$_{11}$O$_{39}$]$^{5-}$ for the oxidative conversion of alkenes to epoxides, aldehydes, or carboxylic acids.[71] The authors demonstrated that depending

on the terminal oxidant used, different oxidation kinetics and selectivities were observed. This allowed the group to propose an initial mechanism which involved oxidation of the {Ru^{III}(H$_2$O)} to a {Ru^V(O)} species which acts as the active oxidation catalyst. While early studies were sometimes affected by the impurity of the typical Ru-precursor RuCl$_3$·xH$_2$O, the use of more well-defined Ru-precursors has firmly established the field of mono-Ru-functionalized POMs.[56] Recent studies have expanded these early studies into energy conversion and demonstrated that the cluster family [Ru^{III}(L)XW$_{11}$O$_{39}$]$^{n-}$ (L = solvent ligand, X = P, Si, Ge) can catalyze the oxidation of water to molecular oxygen in the presence of the chemical oxidant Ce^{IV}.[72,73] In a related study, Fukuzumi and co-workers reported synergistic catalytic effects between SAC and POM-support for water oxidation catalysis.[72] The authors showed that that [Ru^{III}(H$_2$O)GeW$_{11}$O$_{39}$]$^{5-}$ shows higher catalytic performance compared with [Ru^{III}(H$_2$O)SiW$_{11}$O$_{39}$]$^{5-}$ with (NH$_4$)$_2$[Ce^{IV}(NO$_3$)$_6$] (CAN) as a one-electron oxidant in water, highlighting that modification of the internal template (here: GeO$_4$$^{2-}$ vs SiO$_4$$^{2-}$) can be used to modulate SAC/POM-support interactions (**Figure 5**). Mechanistic studies propose that initial oxidative formation of a {Ru^V(O)} species is followed by water-nucleophilic attack (often referred to as WNA mechanism), resulting in the formation of an O—O bond and subsequent release of O$_2$.[72]

Major challenges for using pure POM-SACs in catalytic reactions is their challenging recovery from the reaction mixture, when used under homogeneous conditions, or their low efficiency when used as heterogeneous, solid catalyst. To address this, Wang and co-workers reported the aggregation of Pd-functionalized Class II POM-SACs (K$_{15}$[Pd$_2$(α_2-P$_2$W$_{17}$O$_{61}$)$_2$H]) together with cationic surfactants into different nanostructures, together with their activity for Pd-catalyzed cross-coupling and hydrogenation reactions.[74] However, the study was focused on the effects of the nanostructures formed, while little information was given on the Pd-functionalized POM-SACs system under investigation.
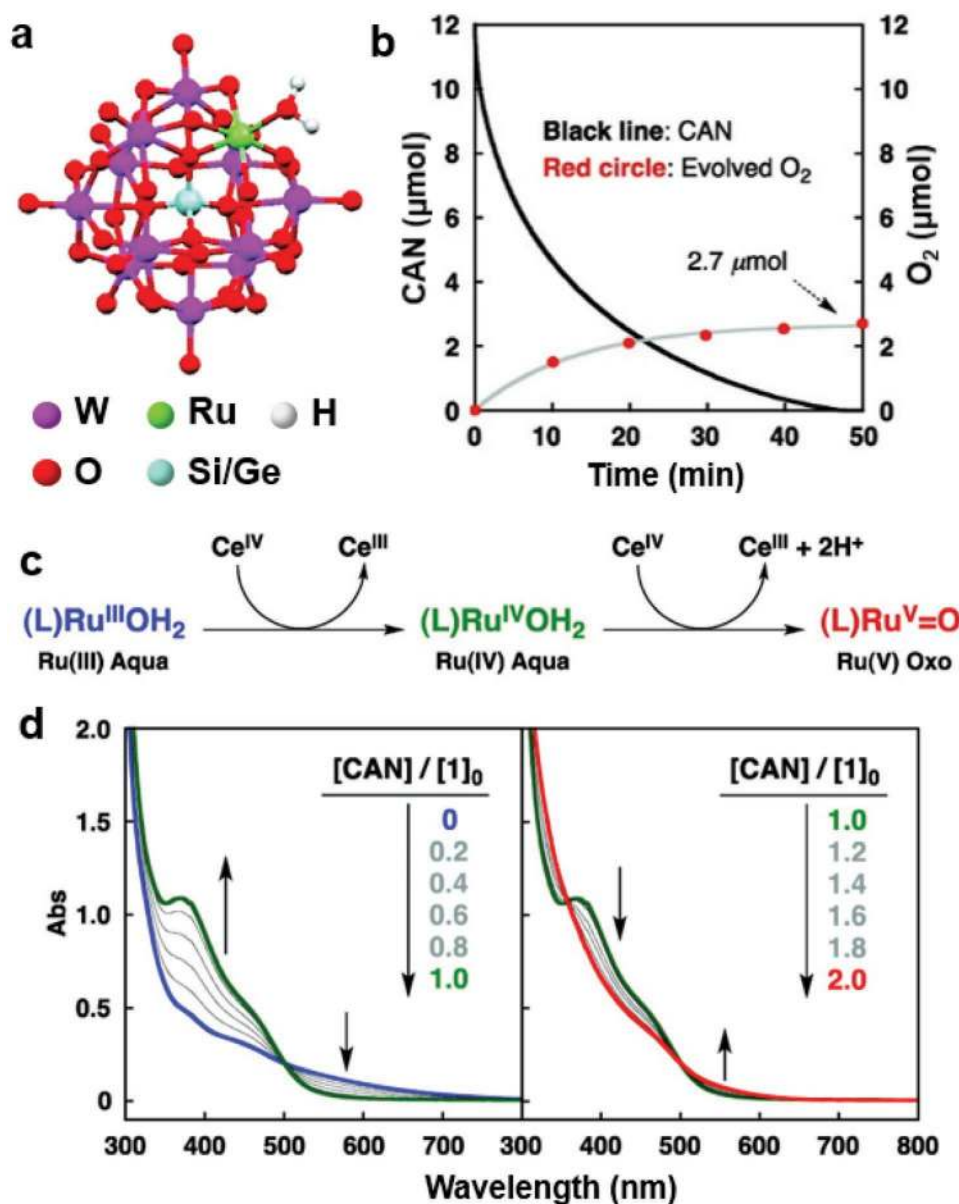
Figure 5. Class II Ru-containing POM-SACs for water oxidation to molecular oxygen. a) Illustration of the virtually isostructural compounds $[Ru^{III}(H_2O)XW_{11}O_{39}]^{5-}$ (X = Si (**1**) or Ge (**2**)). b) Time-dependent changes of the CAN concentration and O_2 evolution for the reaction of **1** with CAN in 0.1 M aqueous HNO_3. c) Schematic illustration of the proposed redox changes of **1** in the initial oxidation steps. d) UV–vis spectral changes of **1** upon addition of different amounts of CAN. Adapted with permission.[72] Copyright 2011, American Chemical Society.

3.3. Non-Noble-Metal-Functionalized POM-SACs

Over the last decade, a major focus in POM chemistry has been the functionalization of lacunary POMs with earth-abundant, redox-active metal ions, often 3d-transition metals.[52] Incorporation of a single metal cation into a lacunary POM structure therefore leads to a Class II POM-SAC. As a prime example, the catalytic activity of the metal-functionalized Class II POM-SACs $[M(H_2O)XW_{11}O_{39}]^{n-}$ (M = Fe^{III}, Mn^{III}; X = P, Si, general structure see Figure 5a) has been studied for the oxidative C−H activation of cyclooctane to give the corresponding alcohol, ketone, or peroxide, using H_2O_2 as terminal oxidant.[75] The authors observed high reactivity for both metal-functionalized

species and noted significant differences in reactivity and selectivity: the silicotungstates showed lower reactivities (in terms of turnover numbers), but higher selectivities for the peroxide species, compared with the phosphotungstates. In addition, the Fe-substituted species showed higher reactivity than the Mn-functionalized POM-SACs.[75] The authors propose that this high reactivity of the Fe-species is due to Fenton-like one-electron activation of H_2O_2 by the native Fe(III) center, which could also explain the high selectivity toward cyclooctyl hydroperoxide observed.

In a different approach, Streb and co-workers used the mono-Cu^{II}-functionalized vanadate $[(Me_2NH_2)Cu(MeCN)V_{12}O_{32}Cl]^{2-}$ (= {**CuV12**}) as a model for Class II POM-SACs to
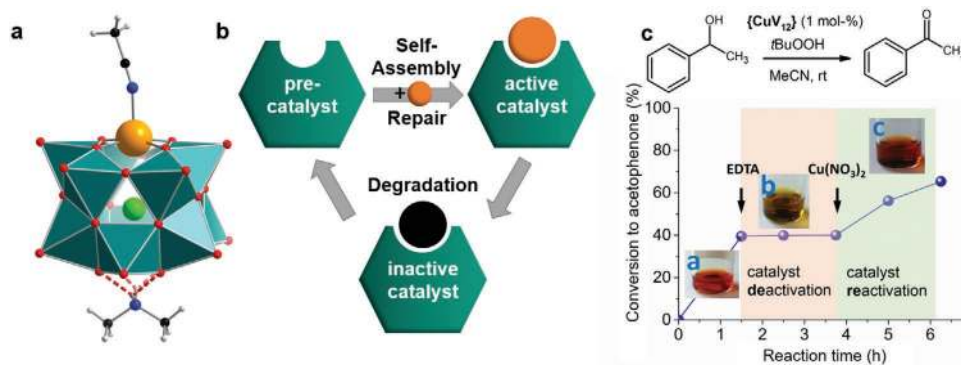
Figure 6. a) Illustration of the POM-SAC **{CuV12}** [(Me₂NH₂)Cu(MeCN)V₁₂O₃₂Cl]²⁻ (Cu: orange, V: teal; O: red; N: blue; C: black; H: white). b) **{CuV12}** catalyst deactivation and repair mechanism; c) catalytic performance of **{CuV12}** for the oxidation of 1-phenylethanol to acetophenone. Catalyst deactivation using Cuᴵᴵ-complexation by EDTA (ethylene diamine tetraacetate). Catalyst repair by addition of Cuᴵᴵ. Reproduced with permission.[76] Copyright 2017, Wiley-VCH.

explore catalyst deactivation and repair (**Figure 6**).[76] The catalytic activity of the system was studied for the selective oxidation of 1-phenylethanol to acetophenone using *t*BuOOH as terminal oxidant. The authors reported that the reactive site is the Cu(II) center that can be removed from the cluster framework by complexing agents (e.g., ethylenediamine tetraacetate, EDTA), resulting in complete loss of catalytic activity. Addition of Cu(II) salts to this reaction solution results in the re-formation of the active **{CuV12}** species, and catalytic activity is recovered.[76]

The systems described above are characterized by typically weakly bound ligands (e.g., solvent molecules) at the SAC site. This is an important feature for the reactivity and stability of these POM-SACs. In consequence, factors, such as ligand binding strength, exchange kinetics, and electronic interactions have significant impact on structure and function of the resulting systems.

3.4. POM-SACs as Models for Reducible Solid-State Metal Oxides

SACs often feature vacant coordination sites which facilitate unusual reactivity and ligand binding behavior, similar to the reactivity of defect sites on solid-state metal oxides. This structural similarity has been exploited in POM-SAC chemistry, where systems featuring redox-active M=O groups, such as V=O, have been established as models for reducible solid-state metal oxides (e.g., V₂O₅), which are important industrial oxidation catalysts.[77] Pioneering work by Neumann has explored their oxygen atom transfer chemistry and oxidation catalysis, with a focus on mono- and multivanadium-functionalized molybdate Keggin POMs H₍₃₊ₓ₎[VₓPMo₍₁₂₋ₓ₎O₄₀] (x = 1, 2, 3), which can be considered POM-single-site catalysts (POM-SSCs, which contain two or more reactive metal centers in the POM framework). Their importance in POM-SACs chemistry will be discussed in Section 4.[78]

More recently, Matson and colleagues have used vanadium oxo-alkoxide clusters of the general formula [V₆O₇(OR)₁₂]ⁿ± (R = organic group, e.g., CH₃) as molecular models to understand the redox-chemistry and surface oxygen removal of these systems (**Figure 7**).[79–81] The group showed that terminal V=O bonds in these clusters can be selectively activated by oxygen

atom transfer using oxophilic O-acceptors. In consequence, removal of an oxygen atom from a {Vⱽ=O} species results in formation of a two-electron reduced {Vᴵᴵᴵ} surface site,[79] similar to the Mars-van Krevelen process proposed for solid-state vanadium oxides.[82]

In a related study, Poblet, Proust, Guillemot and colleagues demonstrated that isolated {Vᴵᴵᴵ(thf)} moieties (thf = tetrahydrofuran solvent ligand) can be stabilized in the W-based lacunary Keggin anion [SbW₉O₃₃(ᵗBuSiO)₃V(thf)]³⁻. Exposure of the system to O₂ revealed the high reactivity of the system and led to a 2-electron oxidation of the V center to form fully oxidized {Vⱽ=O} groups. Notably, 2-electron reduction of the resulting species [SbW₉O₃₃(ᵗBuSiO)₃VO]³⁻ gave a mixed-valent cluster where one electron resided in a vanadium d-orbital (Vᴵⱽ), while the other was localized in a W-based d-orbital (Wⱽ). This is in
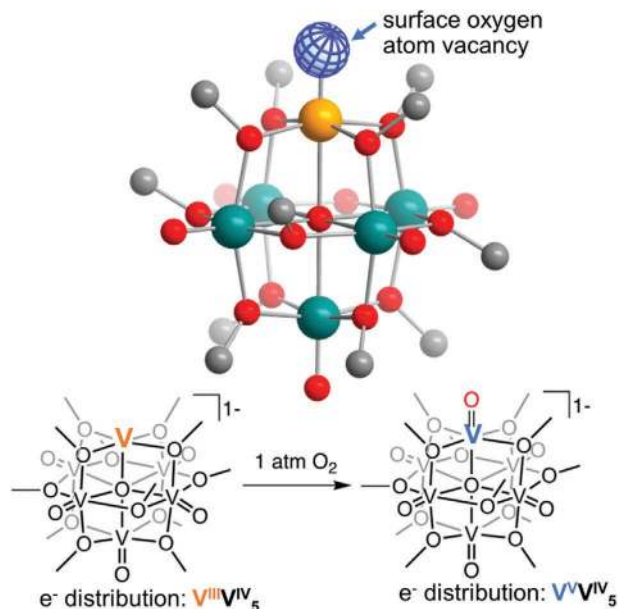
Figure 7. Top: structural representation of the Matson model vanadate highlighting the oxygen atom vacancy on the cluster surface. Bottom: reactivity of the model vanadate for oxygen activation, showing the formal two-electron oxidation of the single-atom vanadium site. Adapted with permission.[79] Copyright 2018, American Chemical Society.

ADVANCED
SCIENCE NEWS
www.advancedsciencenews.com

ADVANCED
ENERGY
MATERIALS
www.advenergymat.de

stark contrast to the original species, where both d-orbital electrons were localized in vanadium d-orbitals (V^{III}). This study highlights that coordination environment control of reactive sites in POM-SACs has enormous impact on their structure and function. Also, the authors describe the system as a reliable model for isolated V^{III} sites, which are key intermediates in Mars-van Krevelen-type oxidation catalyses.[83]

4. Future Directions for POM-SACs

4.1. From POM-Single Atom Catalysts to POM-Single-Site Catalysts

One key property of POMs is their ability to embed one or several reactive metal centers into the POM-framework, thereby enabling the transition from POM-SACs to POM-SSCs,[55,84] which hold great promise for catalysis and energy technologies and will be exemplified briefly.

In the field of energy conversion, the embedding of multiple redox-active metal centers has attracted widespread attention, as the presence of several reaction sites in close proximity can facilitate complex (proton-coupled) multielectron transfers which are difficult to achieve by a single metal site.[85,86] In POM chemistry, prime example is the use of so-called sandwich POMs where several reactive metal ions are coordinated between two stabilizing POM clusters.[57,87–89] In the field of water-to-oxygen oxidation chemistry, this concept has been pioneered by the groups of Bonchio[85] and Hill.[90] The groups embedded a tetraruthenium complex, $[Ru_4O_4(OH)_2(H_2O)_4]^{6+}$, between two lacunary Keggin tungstates $[\gamma\text{-}SiW_{10}O_{36}]^{8-}$, to give the POM-SSC $[Ru_4O_4(OH)_2(H_2O)_4(\gamma\text{-}SiW_{10}O_{36})_2]^{10-}$ (**Figure 8**a). The system is capable of (photo-, electro-) chemical water oxidation to O_2.[91] Experimental and theoretical studies[91] showed that in the native cluster, all Ru centers are in oxidation state +4, and four consecutive 1-electron oxidations to the respective Ru(V) centers is possible.[92] This all-Ru(V)-system is capable of water oxidation following a WNA mechanism.[93] Studies by Prato, Bonchio and colleagues further demonstrated, that deposition of the Ru-functionalized POM-SSCs on carbon

nanotubes is possible, leading to nanostructured composite electrocatalysts for water oxidation catalysis.[94]

Another widely-explored class of POM-SSCs are vanadium-functionalized Keggin POMs of the type $H_{(3+x)}[V_xPMo_{(12-x)}O_{40}]$ (x = 1, 2, 3). These species combine highly oxidation-reactive vanadate centers with the presence of strongly acidic protons bound to the POM surface, making them ideal models for proton-coupled oxidation catalysis.[78,95] The group of Neumann have pioneered the use of the species $H_5[V_2PMo_{10}O_{40}]$ as oxidation catalyst for a range of organic substrate oxidations, ranging from C−H activation to alcohol oxidation and epoxidation.[78] The authors demonstrated that this POM-SSCs can utilize molecular oxygen to catalytically drive substrate oxidations, and that—depending on the reaction system—can follow an outer-sphere electron transfer mechanism or an electron transfer—oxygen transfer mechanism (ET-OT mechanism), involving the reduction of one or two V(V) centers to V(IV) with subsequent proton-coupled reoxidation by O_2, giving H_2O as side-product. Notably, $H_5[V_2PMo_{10}O_{40}]$ is a superior oxidation catalyst compared with the isostructural species $H_3[PMo_{12}O_{40}]$, even so all species have comparable redox properties. Key difference is that typically rate-limiting re-oxidation of V(IV) → V(V) is much faster compared with the Mo(V)→Mo(VI) reoxidation. Given that often, gaseous O_2 is used as reoxidant, chemical engineering approaches are required to maximize O_2 mass transfer to the active catalyst.[96] Intriguingly, there are five structural isomers of $H_5[V_2PMo_{10}O_{40}]$, depending on the relative position of the two V centers in the cluster shell (Figure 8b). While separation of the isomers is so far not established, initial calculations highlight that the isomers differ in their redox-properties.[78] Moreover, a recent study by Neumann and Weinstock highlights that under highly acidic conditions, individual $[VO_2]^+$ units can be released from the $H_5[V_2PMo_{10}O_{40}]$ cluster shell during catalysis to act as reactive sites. When the pH value of the reaction mixture is raised, the original catalyst $H_5[V_2PMo_{10}O_{40}]$ is reformed and can be quantitatively recovered. This work highlights how POM-SACs or POM-SSCs could be utilized for dynamic coordination chemistry and on-demand delivery of reactive molecular species.[97]
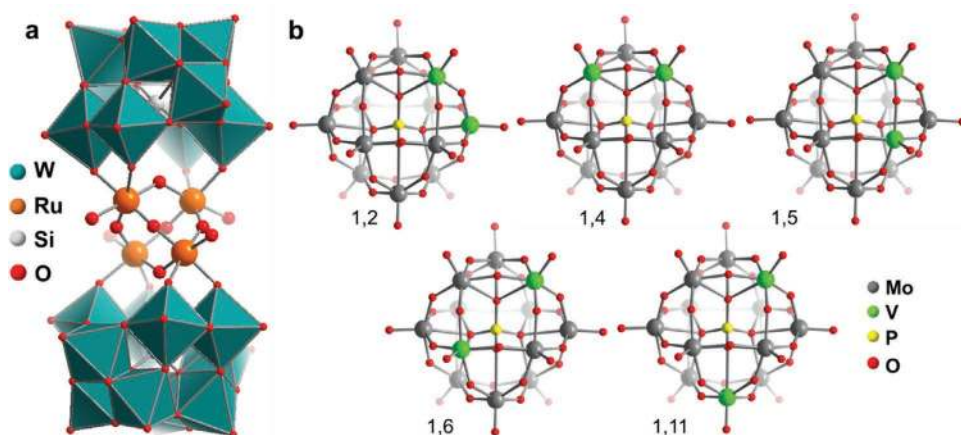


Figure 8. Structures of model POM-SSCs. a) The water oxidation catalyst $[Ru_4O_4(OH)_2(H_2O)_4(\gamma\text{-}SiW_{10}O_{36})_2]^{10-}$.[93] b) Five structural isomers of the oxidation catalyst $H_5[V_2PMo_{10}O_{40}]$.[78]

ADVANCED
SCIENCE NEWS
www.advancedsciencenews.com

ADVANCED
ENERGY
MATERIALS
www.advenergymat.de

4.2. Electrocatalysis

One emerging area of immense potential for POM-SACs is electrocatalysis, where the SAC site together with the POM-support could provide useful properties, e.g., for energy-related small molecule activation (O_2, H_2O, CO_x, N_2, etc.). A major bottleneck for selective molecule activation, particularly in aqueous electrolytes is the competitive binding of different species to the catalyst active site. For reductive activations, such as the N_2 to NH_3 reaction, binding of H-atoms to the catalyst and subsequent competitive H_2 evolution rather than NH_3 formation are critical, as this would lead to low faradaic efficiencies (meaning that the undesired side reaction (H_2 evolution) uses up much of the energy input). To overcome this bottleneck, Liu and co-workers have recently used DFT to systematically study Ru-functionalized Keggin POMs $[XM_{12}O_{40}]^{n-}$ (X = P (n = 3), Si (n = 4), M = W^{VI}, Mo^{VI}) for N_2 reduction.[98] The authors explored the Gibbs free energy change (ΔG) for the adsorption of $*N_2$ and $*H$ on four Keggin-POM-supported Ru single atom electrocatalysts when applying a reductive voltage. The authors reported high nitrogen-binding selectivity for the phosphorus-templated tungstate- and molybdate-Keggin clusters, while the silicon-templated analogues favor hydrogen binding (**Figure 9**). Clearly, these computations proposed intriguing reactivity and reactivity differences for the systems explored, and experimental work is urgently required to assess whether these theoretical studies can be translated into experimental catalysis.[98]

Following a related line of research, Liu and colleagues explored whether Class II POM-SACs could also have importance for N_2 activation. To this end, the authors studied N_2-complexes of the metal-functionalized Keggin anion $[M(N_2)PW_{11}O_{39}]^{5-}$ (M = Mo^{II}, Tc^{II}, W^{II}, Re^{II}, and Os^{II}), and calculated that these systems show a Jahn–Teller distortion at the M sites which leads to an effective orbital mixture between σ_{2s}^* orbital of N_2 and d_z^2 metal orbitals.[62] As a result, the authors proposed
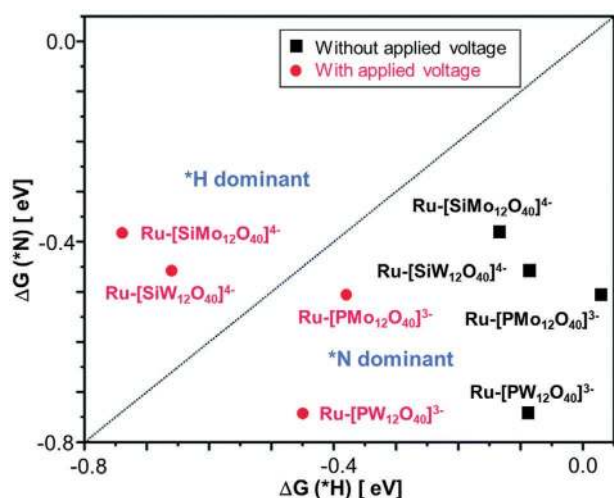
that these systems (if/when they are synthetically accessible), could be viable N_2 activation catalysts.

A novel top-down POM-based SAC design approach has recently been reported by Streb, Liu and colleagues: the group demonstrated how immobilization of POM-SSCs on high surface-area electrically conductive carbon can be achieved at high loading. In detail, the Keggin-polyoxomolybdate $[PMo_{12}O_{40}]^{3-}$ was used as precursor to deposit POM-like molybdenum(VI)-oxo sub-nanometer clusters ($[Mo\text{-}oxo]_n$, n = 1–20) on high surface-area mesoporous carbon.[99] The material showed excellent performance for electrocatalytic ORR, in part superior to a commercial Pt/C material. Given the wide chemical tunability of POMs, this approach could be amenable for the top-down deposition of POM-SACs and POM-SSCs, and thereby open new avenues for facile materials design. In later studies, the authors also demonstrated that the system is suitable for deposition on screen-printed electrodes as a sensitive and selective electrochemical H_2O_2 sensor, demonstrating the wide scope of these materials.[100] In a related study, Zhang, Fan and co-workers developed a dual-atom catalyst consisting of O-bridged W-Mo atoms anchored to N-doped graphene vacancies through oxygen atoms with W—O—Mo—O—C configuration. The material was synthesized by controlled self-assembly followed by nitridation. This W-Mo heterodimer catalyst enables Pt-like activity and ultrahigh stability for HER over a wide pH range, showing higher activity compared with similarly structured Mo–Mo and W–W homodimer catalysts.[101] In another insightful study, Wagberg, Tan and colleagues prepared sub-nanometer heterometallic CoW and FeCoW clusters via a molecule-to-cluster strategy by using different POMs (i.e., $[\{Co_4(OH)_3PO_4\}_4(SiW_9O_{34})_4]^{32-}$, $[\{Fe_2Co_2(OH)_3PO_4\}_4(SiW_9O_{34})_4]^{24-}$, and $[\{FeCo_3(OH)_3PO_4\}_4(SiW_9O_{34})_4]^{28-}$) as precursors. The authors noted that the Fe content in the FeCoW clusters can simply be controlled by employing POM precursors containing different numbers of Fe atoms. The most promising system studied featured excellent OER activity with η_{10} = 192 mV and a low Tafel slope of 36 mV dec^{-1}.[102]

4.3. Light-Driven Catalysis

SACs and SSCs have been successfully established for light-driven catalysis,[55] particularly with a view of solar energy conversion and usage for small molecule activation in sustainable energy, e.g., H_2 production, CO_2 reduction, and N_2 reduction.[103] Similarly, POMs are well-established light-driven catalysts with photoactivity in the UV and visible spectral range, with applications ranging from light-driven organic substrate oxidation to water oxidation and hydrogen evolution.[47,85,104] To-date, only few examples of POM-SACs for light-driven catalysis have been reported. In a pioneering example,[105] the mono-cobalt-functionalized species $[Co(H_2O)_2(\gamma\text{-}SiW_{10}O_{35})_2]^{10-}$ has been combined with the visible-light-driven photosensitizer $[Ru(bpy)_3]^{2+}$ (bpy = 2,2′-bipyridine) and the terminal oxidant $S_2O_8^{2-}$ to enable light-driven single-site water oxidation. The authors reported that under their conditions (aqueous borate buffer, pH 9.0), the cluster shows hydrolytic stability and they concluded that the catalytic activity is in fact caused by $[Co(H_2O)_2(\gamma\text{-}SiW_{10}O_{35})_2]^{10-}$ and not by possible degradation products (e.g., cobalt oxide/hydroxide materials).

Figure 9. Calculated $\Delta G(*N_2)$ and $\Delta G(*H)$ for Ru-[SiMo$_{12}$O$_{40}$]$^{4-}$, Ru-[SiW$_{12}$O$_{40}$]$^{4-}$, Ru-[PMo$_{12}$O$_{40}$]$^{3-}$, and Ru-[PW$_{12}$O$_{40}$]$^{3-}$ with and without applied voltage. The dashed line indicates $\Delta G(*N_2)$ = $\Delta G(*H)$. Adapted with permission.[98] Copyright 2020, Royal Society of Chemistry.

4.4. Gas-Phase Catalysis

Metal oxide clusters have been pioneered as gas-phase model systems to explore gas–solid catalytic processes including CH-bond activation and CO oxidation.[106] Very recently, Yan and co-workers reported that POM-SACs can be used as gas-phase models to study reaction mechanisms, e.g., for CO and alcohol oxidation.[107] The group used high-resolution electrospray ionization mass spectrometry together with DFT calculations to explore mechanisms, reaction intermediates as well as kinetic and thermodynamic properties. The study demonstrates that the use of POM-SACs as model catalysts, together with combined cutting-edge experimental and theoretical methods lead to unprecedented levels of insight into complex reaction pathways.

4.5. Enantioselective Catalysis

Another area where POM-SACs and POM-SSCs could become interesting catalyst models is in the field of enantioselective catalysis.[108,109] Pioneering work has already demonstrated the ability to localize SSCs in chiral environments on surfaces and inside pores. This has enabled ground-breaking applications in heterogeneous organic enantioselective synthesis with applications in pharmaceutical chemistry or agrochemistry.[110] In POM chemistry, the formation of chiral POM clusters is well-established.[111,112] Often, racemic mixtures of chiral POMs form by spontaneous symmetry breaking during self-assembly, so that subsequent separation steps are required to separate the stereoisomers, which is still a challenge. However, if more straight-forward routes to chiral POMs as well as their metal functionalization can be established, this would open vast new opportunities for POM-SACs or POM-SSCs development where the reactive metal sites as well as the chiral POM framework could act in unison to perform enantioselective (electro-/photo-)catalytic processes for sustainable organic syntheses.

4.6. Harnessing SAC/POM-Support Interactions

POMs are ideal models to explore SAC-support interactions and to learn how modification of the support can alter the reactivity of the SAC. Prime example are derivatives of the Keggin anion $[XM_{12}O_{40}]^{n-}$, where modification of the internal template X (e.g., B, Si, P, etc.) and/or the metal M (e.g., Mo, W, V, and mixtures thereof) offer ample opportunity to systematically explore this field.[53] In addition, these studies could shed light on dual-site catalysts where not only the SAC but also the POM framework can engage in catalytic processes (including light-driven systems or redox-conversions), so that the functional synergy between both components can be harnessed for novel, possibly even multifunctional molecular systems.[60] In addition, we currently lack detailed understanding of the reactivity differences between Class I and Class II POM-SACs based on the differences in binding mode and adsorption energies of the SAC metals. Tuning POM structure and SAC binding could open new avenues to optimize reactivity by providing strong metal–support interaction to resist catalyst aggregation, while optimizing substrate or electrolyte interactions to provide fast and stable reaction kinetics.[60] For these challenging tasks, advanced in situ/operando characterization methods together with high-level computational analyses are required to gain molecular-level understanding. POM-SACs are ideal for these studies, as their molecular nature provides an ensemble of molecules where each SAC atom is in an identical chemical environment. This results in ideal systems to provide unprecedented mechanistic insights.[53]

5. Summary and Conclusion

This Review summarizes how molecular metal oxides—polyoxometalates—can be harnessed as molecular supports for single atom catalysts, giving the emerging molecular compound class of POM-SACs. These model systems are ideally suited to address fundamental SAC research questions including SAC agglomeration, reversible deposition, and leaching under operation. In addition, early studies highlight the role of POM-SAC in energy relevant applications, such as water splitting or CO_x activation. While this research field is still in its infancy, the possibilities of combining well-defined molecular model systems with high level experimental and theoretical studies paves the way for new designer SACs for globally important chemical challenges in catalysis and energy technologies. Analysis of potential future research directions shows that POM-SACs are of high relevance for light-driven catalysis or electrocatalysis as well as the activation of small, inert molecules.

Conflict of Interest

The authors declare no conflict of interest.

[1] L. Liu, A. Corma, *Chem. Rev.* **2018**, *118*, 4981.
[2] X. F. Yang, A. Wang, B. Qiao, J. Li, J. Liu, T. Zhang, *Acc. Chem. Res.* **2013**, *46*, 1740.

ADVANCED
SCIENCE NEWS

www.advancedsciencenews.com

ADVANCED
ENERGY
MATERIALS

www.advenergymat.de

[3] Z. Li, S. Ji, Y. Liu, X. Cao, S. Tian, Y. Chen, Z. Niu, Y. Li, *Chem. Rev.* **2020**, *120*, 623.

[4] Y. Wang, J. Mao, X. Meng, L. Yu, D. Deng, X. Bao, *Chem. Rev.* **2019**, *119*, 1806.

[5] C. Zhao, X. Dai, T. Yao, W. Chen, X. Wang, J. Wang, J. Yang, S. Wei, Y. Wu, Y. Li, *J. Am. Chem. Soc.* **2017**, *139*, 8078.

[6] Y. Chen, S. Ji, Y. Wang, J. Dong, W. Chen, Z. Li, R. Shen, L. Zheng, Z. Zhuang, D. Wang, Y. Li, *Angew. Chem., Int. Ed.* **2017**, *56*, 6937.

[7] J. Liu, *ACS Catal.* **2017**, *7*, 34.

[8] S. Liang, C. Hao, Y. Shi, *ChemCatChem* **2015**, *7*, 2559.

[9] S. Ji, Y. Chen, X. Wang, Z. Zhang, D. Wang, Y. Li, *Chem. Rev.* **2020**, *120*, 11900.

[10] H.-Y. Zhuo, X. Zhang, J.-X. Liang, Q. Yu, H. Xiao, J. Li, *Chem. Rev.* **2020**, *120*, 12315.

[11] Y. Peng, B. Lu, S. Chen, *Adv. Mater.* **2018**, *30*, 1.

[12] L. Nie, D. Mei, H. Xiong, B. Peng, Z. Ren, X. I. P. Hernandez, A. DeLaRiva, M. Wang, M. H. Engelhard, L. Kovarik, A. K. Datye, Y. Wang, *Science* **2017**, *358*, 1419.

[13] M. Moses-Debusk, M. Yoon, L. F. Allard, D. R. Mullins, Z. Wu, X. Yang, G. Veith, G. M. Stocks, C. K. Narula, *J. Am. Chem. Soc.* **2013**, *135*, 12634.

[14] M. Babucci, A. Guntida, B. C. Gates, *Chem. Rev.* **2020**, *120*, 11956.

[15] S. M. J. Rogge, A. Bavykina, J. Hajek, H. Garcia, A. I. Olivos-Suarez, A. Sepulveda-Escribano, A. Vimont, G. Clet, P. Bazin, F. Kapteijn, M. Daturi, E. V. Ramos-Fernandez, F. X. Llabres i Xamena, V. Van Speybroeck, J. Gascon, *Chem. Soc. Rev.* **2017**, *46*, 3134.

[16] Z. Liang, C. Qu, D. Xia, R. Zou, Q. Xu, *Angew. Chem., Int. Ed.* **2018**, *57*, 9604.

[17] T. Sun, L. Xu, D. Wang, Y. Li, *Nano Res.* **2019**, *12*, 2067.

[18] L. Jiao, H. L. Jiang, *Chem* **2019**, *5*, 786.

[19] C. Wan, X. Duan, Y. Huang, *Adv. Energy Mater.* **2020**, *10*, 1903815.

[20] A. P. Côté, A. I. Benin, N. W. Ockwig, M. O'Keeffe, A. J. Matzger, O. M. Yaghi, *Science* **2005**, *310*, 1166.

[21] X. Feng, X. Ding, D. Jiang, *Chem. Soc. Rev.* **2012**, *41*, 6010.

[22] J. Li, M. F. Stephanopoulos, Y. Xia, *Chem. Rev.* **2020**, *120*, 11699.

[23] Q. Fu, H. Saltsburg, M. Flytzani-Stephanopoulos, *Science* **2003**, *301*, 935.

[24] B. Qiao, A. Wang, X. Yang, L. F. Allard, Z. Jiang, Y. Cui, J. Liu, J. Li, T. Zhang, *Nat. Chem.* **2011**, *3*, 634.

[25] W. Zhu, C. Chen, *Chem* **2019**, *5*, 2737.

[26] Y. Chen, S. Ji, C. Chen, Q. Peng, D. Wang, Y. Li, *Joule* **2018**, *2*, 1242.

[27] Y. Wang, H. Su, Y. He, L. Li, S. Zhu, H. Shen, P. Xie, X. Fu, G. Zhou, C. Feng, D. Zhao, F. Xiao, X. Zhu, Y. Zeng, M. Shao, S. Chen, G. Wu, J. Zeng, C. Wang, *Chem. Rev.* **2020**, *120*, 12217.

[28] C. Gao, J. Low, R. Long, T. Kong, J. Zhu, Y. Xiong, *Chem. Rev.* **2020**, *120*, 12175.

[29] C. Zhu, S. Fu, Q. Shi, D. Du, Y. Lin, *Angew. Chem., Int. Ed.* **2017**, *56*, 13944.

[30] X. Su, X. F. Yang, Y. Huang, B. Liu, T. Zhang, *Acc. Chem. Res.* **2019**, *52*, 656.

[31] H. Fei, J. Dong, M. J. Arellano-Jiménez, G. Ye, N. Dong Kim, E. L. G. Samuel, Z. Peng, Z. Zhu, F. Qin, J. Bao, M. J. Yacaman, P. M. Ajayan, D. Chen, J. M. Tour, *Nat. Commun.* **2015**, *6*, 8668.

[32] P. Liu, Y. Zhao, R. Qin, S. Mo, G. Chen, L. Gu, D. M. Chevrier, P. Zhang, Q. Guo, D. Zang, B. Wu, *Science* **2016**, *352*, 797.

[33] J. Wang, T. Xia, L. Wang, X. Zheng, Z. Qi, C. Gao, J. Zhu, Z. Li, H. Xu, Y. Xiong, *Angew. Chem., Int. Ed.* **2018**, *57*, 16447.

[34] X. Wu, H. Zhang, J. Dong, M. Qiu, J. Kong, Y. Zhang, Y. Li, G. Xu, J. Zhang, J. Ye, *Nano Energy* **2018**, *45*, 109.

[35] B. H. Lee, S. Park, M. Kim, A. K. Sinha, S. C. Lee, E. Jung, W. J. Chang, K. S. Lee, J. H. Kim, S. P. Cho, H. Kim, K. T. Nam, T. Hyeon, *Nat. Mater.* **2019**, *18*, 620.

[36] P. Huang, J. Huang, S. A. Pantovich, A. D. Carl, T. G. Fenton, C. A. Caputo, R. L. Grimm, A. I. Frenkel, G. Li, *J. Am. Chem. Soc.* **2018**, *140*, 16042.

[37] M. J. Hülsey, J. Zhang, N. Yan, *Adv. Mater.* **2018**, *30*, 1802304.

[38] R. Qin, P. Liu, G. Fu, N. Zheng, *Small Methods* **2018**, *2*, 1.

[39] S. F. J. Hackett, R. M. Brydson, M. H. Gass, I. Harvey, A. D. Newman, K. Wilson, A. F. Lee, *Angew. Chem.* **2007**, *119*, 8747.

[40] X. Guo, G. Fang, G. Li, H. Ma, H. Fan, L. Yu, C. Ma, X. Wu, D. Deng, M. Wei, D. Tan, R. Si, S. Zhang, J. Li, L. Sun, Z. Tang, X. Pan, X. Bao, *Science* **2014**, *344*, 616.

[41] B. Qiao, J. Liu, Y. G. Wang, Q. Lin, X. Liu, A. Wang, J. Li, T. Zhang, J. Liu, *ACS Catal.* **2015**, *5*, 6249.

[42] Y. Pan, S. Liu, K. Sun, X. Chen, B. Wang, K. Wu, X. Cao, W. C. Cheong, R. Shen, A. Han, Z. Chen, L. Zheng, J. Luo, Y. Lin, Y. Liu, D. Wang, Q. Peng, Q. Zhang, C. Chen, Y. Li, *Angew. Chem., Int. Ed.* **2018**, *57*, 8614.

[43] N. Cheng, L. Zhang, K. Doyle-Davis, X. Sun, *Single-Atom Catalysts: From Design to Application*, Springer, Singapore **2019**.

[44] M. T. Pope, A. Müller, *Angew. Chem.* **1991**, *103*, 56.

[45] L. Cronin, A. Müller, *Chem. Soc. Rev.* **2012**, *41*, 7333.

[46] C. L. Hill, C. M. Prosser-McCartha, *Coord. Chem. Rev.* **1995**, *143*, 407.

[47] C. Streb, *Dalton Trans.* **2012**, *41*, 1651.

[48] E. Coronado, C. J. Gómez-García, C. J. Go, *Chem. Rev.* **1998**, *98*, 273.

[49] D. L. Long, R. Tsunashima, L. Cronin, *Angew. Chem., Int. Ed.* **2010**, *49*, 1736.

[50] A. Proust, R. Thouvenot, P. Gouzerh, *Chem. Commun.* **2008**, 1837.

[51] M. T. Pope, *Heteropoly and Isopoly Oxometalates*, Springer-Verlag Berlin, New York **1983**.

[52] A. Kondinski, T. N. Parac-Vogt, *Front. Chem.* **2018**, *6*, 346.

[53] M. J. Hülsey, B. Zhang, Z. Ma, H. Asakura, D. A. Do, W. Chen, T. Tanaka, P. Zhang, Z. Wu, N. Yan, *Nat. Commun.* **2019**, *10*, 1330.

[54] X. López, J. J. Carbó, C. Bo, J. M. Poblet, *Chem. Soc. Rev.* **2012**, *41*, 7537.

[55] J. M. Thomas, *Proc. R. Soc. A: Math. Phys. Eng. Sci.* **2012**, *468*, 1884.

[56] N. V. Izarova, M. T. Pope, U. Kortz, *Angew. Chem., Int. Ed.* **2012**, *51*, 9492.

[57] P. Putaj, F. Lefebvre, *Coord. Chem. Rev.* **2011**, *255*, 1642.

[58] B. Zhang, H. Asakura, J. Zhang, J. Zhang, S. De, N. Yan, *Angew. Chem., Int. Ed.* **2016**, *55*, 8319.

[59] B. Zhang, H. Asakura, N. Yan, *Ind. Eng. Chem. Res.* **2017**, *56*, 3578.

[60] B. Zhang, G. Sun, S. Ding, H. Asakura, J. Zhang, P. Sautet, N. Yan, *J. Am. Chem. Soc.* **2019**, *141*, 8185.

[61] C.-G. Liu, M.-X. Jiang, Z.-M. Su, *Inorg. Chem.* **2017**, *56*, 10496.

[62] Y. Wang, X. M. Chen, L. L. Zhang, C. G. Liu, *Inorg. Chem.* **2019**, *58*, 7852.

[63] L. Gao, F. Wang, M. A. Yu, F. Wei, J. Qi, S. Lin, D. Xie, *J. Mater. Chem. A* **2019**, *7*, 19838.

[64] C. G. Liu, C. Sun, M. X. Jiang, L. L. Zhang, M. J. Sun, *Phys. Chem. Chem. Phys.* **2019**, *21*, 9975.

[65] L. L. Zhang, X. M. Chen, C. G. Liu, *Inorg. Chem.* **2019**, *58*, 5221.

[66] C. G. Liu, Y. J. Chu, L. L. Zhang, C. Sun, J. Y. Shi, *Environ. Sci. Technol.* **2019**, *53*, 12893.

[67] C.-G. Liu, L.-L. Zhang, X.-M. Chen, *Dalton Trans.* **2019**, *48*, 6228.

[68] S. Wang, Y. Feng, S. Lin, H. Guo, *RSC Adv.* **2017**, *7*, 24925.

[69] L.-L. Zhang, M.-J. Sun, C.-G. Liu, *Mol. Catal.* **2019**, *462*, 37.

[70] M. A. Yu, Y. Feng, L. Gao, S. Lin, *Phys. Chem. Chem. Phys.* **2018**, *20*, 20661.

[71] R. Neumann, C. Abu-Gnim, *J. Am. Chem. Soc.* **1990**, *112*, 6025.

[72] M. Murakami, D. Hong, T. Suenobu, S. Yamaguchi, T. Ogura, S. Fukuzumi, *J. Am. Chem. Soc.* **2011**, *133*, 11605.

[73] M. Sadakane, N. Rinn, S. Moroi, H. Kitatomi, T. Ozeki, M. Kurasawa, M. Itakura, S. Hayakawa, K. Kato, M. Miyamoto, S. Ogo, Y. Ide, T. Sano, *Z. Anorg. Allg. Chem.* **2011**, *637*, 1467.

[74] P. He, B. Xu, X. Xu, L. Song, X. Wang, *Chem. Sci.* **2016**, *7*, 1011.

[75] M. S. S. Balula, I. C. M. S. Santos, M. M. Q. Simões, M. G. P. M. S. Neves, J. A. S. Cavaleiro, A. M. V. Cavaleiro, *J. Mol. Catal. A: Chem.* **2004**, *222*, 159.

[76] K. Kastner, M. Lechner, S. Weber, C. Streb, *ChemistrySelect* **2017**, *2*, 5542.

2101120 (12 of 13)

[77] R. R. Langeslay, D. M. Kaphan, C. L. Marshall, P. C. Stair, A. P. Sattelberger, M. Delferro, *Chem. Rev.* **2019**, *119*, 2128.

[78] R. Neumann, *Inorg. Chem.* **2010**, *49*, 3594.

[79] B. E. Petel, W. W. Brennessel, E. M. Matson, *J. Am. Chem. Soc.* **2018**, *140*, 8424.

[80] E. Schreiber, B. E. Petel, E. M. Matson, *J. Am. Chem. Soc.* **2020**, *142*, 9915.

[81] B. E. Petel, E. M. Matson, *Inorg. Chem.* **2020**, https://doi.org/10.1021/acs.inorgchem.0c02052.

[82] C. Doornkamp, V. Ponec, *J. Mol. Catal. A: Chem.* **2000**, *162*, 19.

[83] T. Zhang, A. Solé-Daura, S. Hostachy, S. Blanchard, C. Paris, Y. Li, J. J. Carbó, J. M. Poblet, A. Proust, G. Guillemot, *J. Am. Chem. Soc.* **2018**, *140*, 14903.

[84] J. D. A. Pelletier, J.-M. Basset, *Acc. Chem. Res.* **2016**, *49*, 664.

[85] A. Sartorel, M. Carraro, F. M. Toma, M. Prato, M. Bonchio, *Energy Environ. Sci.* **2012**, *5*, 5592.

[86] H. Dau, C. Limberg, T. Reier, M. Risch, S. Roggan, P. Strasser, *ChemCatChem* **2010**, *2*, 724.

[87] S. T. Zheng, G. Y. Yang, *Chem. Soc. Rev.* **2012**, *41*, 7623.

[88] Q. Han, Y. Ding, *Dalton Trans.* **2018**, *47*, 8180.

[89] M. Blasco-Ahicart, J. Soriano-Lopez, J. J. Carbo, J. M. Poblet, J. R. Galan-Mascaros, *Nat. Chem.* **2018**, *10*, 24.

[90] H. Lv, Y. V. Geletii, C. Zhao, J. W. Vickers, G. Zhu, Z. Luo, J. Song, T. Lian, D. G. Musaev, C. L. Hill, *Chem. Soc. Rev.* **2012**, *41*, 7572.

[91] D. Gao, I. Trentin, L. Schwiedrzik, L. González, C. Streb, *Molecules* **2020**, *25*, 157.

[92] C. Y. Lee, S. X. Guo, A. F. Murphy, T. McCormac, J. Zhang, A. M. Bond, G. Zhu, C. L. Hill, Y. V. Geletii, *Inorg. Chem.* **2012**, *51*, 11521.

[93] S. Piccinin, A. Sartorel, G. Aquilanti, A. Goldoni, M. Bonchio, S. Fabris, *Proc. Natl. Acad. Sci. USA* **2013**, *110*, 4917.

[94] F. M. Toma, A. Sartorel, M. Iurlo, M. Carraro, P. Parisse, C. MacCato, S. Rapino, B. R. Gonzalez, H. Amenitsch, T. Da Ros, L. Casalis, A. Goldoni, M. Marcaccio, G. Scorrano, G. Scoles, F. Paolucci, M. Prato, M. Bonchio, *Nat. Chem.* **2010**, *2*, 826.

[95] S. Wang, G. Yang, *Chem. Rev.* **2015**, *115*, 4893.

[96] M. Lechner, R. Güttel, C. Streb, *Dalton Trans.* **2016**, *45*, 16716.

[97] C. K. Tiwari, M. Baranov, A. Neyman, R. Neumann, I. A. Weinstock, *Inorg. Chem.* **2020**, *59*, 11945.

[98] L. Lin, L. Gao, K. Xie, R. Jiang, S. Lin, *Phys. Chem. Chem. Phys.* **2020**, *22*, 7234.

[99] R. Liu, K. Cao, A. H. Clark, P. Lu, M. Anjass, J. Biskupek, U. Kaiser, G. Zhang, C. Streb, *Chem. Sci.* **2020**, *11*, 1043.

[100] R. Liu, Y. Luo, Y. Zheng, G. Zhang, C. Streb, *Chem. Commun.* **2020**, *56*, 9465.

[101] Y. Yang, Y. Yang, Y. Qian, H. Li, Z. Zhang, Y. Mu, D. Do, B. Zhou, J. Dong, W. Yan, Y. Qin, L. Fang, R. Feng, J. Zhou, P. Zhang, J. Dong, G. Yu, Y. Liu, X. Zhang, X. Zhang, X. Fan, X. Fan, *Sci. Adv.* **2020**, *6*, eaba6586.

[102] X. B. Han, X. Y. Tang, Y. Lin, E. Gracia-Espino, S. G. Liu, H. W. Liang, G. Z. Hu, X. J. Zhao, H. G. Liao, Y. Z. Tan, T. Wagberg, S. Y. Xie, L. S. Zheng, *J. Am. Chem. Soc.* **2019**, *141*, 232.

[103] B. Xia, Y. Zhang, J. Ran, M. Jaroniec, S.-Z. Qiao, *ACS Cent. Sci.* **2021**, *7*, 39.

[104] G. Paille, A. Boulmier, A. Bensaid, M. H. Ha-Thi, T. T. Tran, T. Pino, J. Marrot, E. Rivière, C. H. Hendon, O. Oms, M. Gomez-Mingot, M. Fontecave, C. Mellot-Draznieks, A. Dolbecq, P. Mialane, *Chem. Commun.* **2019**, *55*, 4166.

[105] R. Xiang, Y. Ding, J. Zhao, *Chem. Asian J.* **2014**, *9*, 3228.

[106] H. Schwarz, *Angew. Chem., Int. Ed.* **2015**, *54*, 10090.

[107] M. J. Hülsey, G. Sun, P. Sautet, N. Yan, *Angew. Chem., Int. Ed.* **2021**, *60*, 4764.

[108] H. An, Y. Zhang, Y. Hou, T. Hu, W. Yang, S. Chang, J. Zhang, *Dalton Trans.* **2018**, *47*, 9079.

[109] W. J. Xuan, C. Botuha, B. Hasenknopf, S. Thorimbert, *Chem. - Eur. J.* **2015**, *21*, 16512.

[110] J. M. Thomas, R. Raja, *Acc. Chem. Res.* **2008**, *41*, 708.

[111] B. Hasenknopf, K. Micoine, E. Lacôte, S. Thorimbert, M. Malacria, R. Thouvenot, *Eur. J. Inorg. Chem.* **2008**, 5001.

[112] D. Y. Du, L. K. Yan, Z. M. Su, S. L. Li, Y. Q. Lan, E. B. Wang, *Coord. Chem. Rev.* **2013**, *257*, 702.

Rongji Liu obtained his Ph.D. in 2014 from the Institute of Process Engineering, Chinese Academy of Sciences. He is currently senior postdoc at Helmholtz Institute Ulm, Germany. His research interests are focused on the preparation of POM-based functional materials and composites for challenging reactions in energy research and electrocatalysis, including water splitting and small molecule activation.

Carsten Streb is professor of Inorganic Chemistry at Ulm University and group leader at the Helmholtz-Institute Ulm. His love for POMs started during his Ph.D., working with Lee Cronin at the University of Glasgow. His current research is focused on designing POM-based functional materials and composites to address global chemical challenges including energy conversion/storage, water purification, and public health.